

Determination of Earth rotation variations by means of VLBI and GPS and comparison to conventional models



Sigrid English, Paulo Jorge Mendes Cerveira, Robert Weber, Harald Schuh

Abstract

Oceanic and solid Earth tides induce periodic signals in the Earth rotation parameters (ERP), i.e., the pole coordinates (x_p , y_p) and universal time (UT1) or length of day (LOD), respectively. The oceanic tides cause variations with diurnal and semidiurnal periods in all parameters, whereas the zonal Earth tides mainly influence the rotational speed of the Earth, and thus UT1 and LOD. These signals show periods from ~ 5 days to 18.6 years. Today, the ERP and their variations can be observed by modern space geodetic techniques with an unprecedented accuracy and temporal resolution. For the investigation of short and long period tidal effects ERP series of one year were computed from GPS observational data with hourly and 6-hours intervals. One ERP series with daily resolution was generated from six years of VLBI observations. The high-resolution GPS-based ERP series was analysed w.r.t. daily and sub-daily tidal variations. The variations in the VLBI-based dUT1 series and the GPS-based LOD series of lower temporal resolution were examined for periods from 5 to 32 days. The observed periods and corresponding amplitudes were compared to the theory of tidal excitation in order to reveal and, if possible, interpret remaining fluctuations in the ERP series. We retrieved significant signal peaks at the periods of the major tidal constituents, as well as at non-tidal periods from 5 to 32 days. The occurrence of the unexpected variations is supposed to be primarily a consequence of insufficient modelling of the atmospheric excitation.

Kurzfassung

Die Gezeiten der festen Erde und der Ozeane verursachen periodische Schwankungen der Erdrotationsparameter (ERP), d.h. der Polkoordinaten (x_p , y_p) und der Weltzeit (UT1), beziehungsweise deren zeitlicher Ableitung, der Tageslänge (LOD). Die Meeresgezeiten bewirken eintägige und halbtägige Variationen in allen Parametern, während die zonalen Erdgezeiten vorwiegend die Rotationsgeschwindigkeit der Erde und damit UT1 und LOD beeinflussen. Diese Effekte haben Perioden von ~ 5 Tagen bis zu 18,6 Jahren. Die ERP und ihre Änderungen können heute in hoher zeitlicher Auflösung mit modernen geodätischen Weltraumverfahren beobachtet werden. Zur Betrachtung der kurz- und langperiodischen Gezeiteffekte wurden ERP-Zeitreihen mit einstündiger und 6-stündiger Auflösung aus GPS-Beobachtungen eines Jahres generiert. Aus VLBI-Beobachtungsdaten von sechs Jahren wurden ERP, mit zeitlicher Auflösung von 24 Stunden berechnet. Die hochauflösende GPS-basierte ERP-Serie wurde bezüglich täglicher und subtäglicher Variationen analysiert. Schwankungen in der VLBI-basierten dUT1 und in der GPS-basierten LOD-Serie wurden auf Perioden von 5 bis 32 Tagen untersucht. Die beobachteten Perioden und die dazugehörigen Amplituden wurden mit theoretischen Modellen für die Anregung durch Gezeiten verglichen, um verbleibende Fluktuationen in den ERP-Serien aufzudecken und gegebenenfalls zu interpretieren. Signifikante Signale wurden sowohl mit Perioden der Hauptgezeiterme, als auch mit nicht gezeitenbezogenen Perioden, im langperiodischen Bereich von 5 bis 32 Tagen, gefunden. Das Auftreten der unerwarteten Variationen ist vermutlich eine Folge unzureichender Modellierung der atmosphärischen Anregung.

1. Introduction

The rotational behaviour of the Earth is highly connected to various geophysical processes. We distinguish between two sets of parameters for describing Earth rotation. The direction of the rotation axis in an Earth-fixed system is expressed by two parameters x_p and y_p , their variation is called polar motion (PM). The parameter dUT1, which is the difference between universal time UT1 and UTC (universal time coordinated), gives access to variations of the rotational speed of the Earth. The three parameters x_p , y_p and dUT1 are

called Earth rotation parameters (ERP). Depending on the purpose, also the time derivative of dUT1, i.e., the length of day (LOD) is assigned to this parameter set. Earth rotation variations of geodynamic origin are typically studied by observing the Earth rotation parameters. The ERP together with precession-nutation form the Earth orientation parameters (EOP). The EOP are the linking elements between celestial and terrestrial reference frames, i.e., they are transformation arguments. This transformation could in principle be reduced to an arbitrary spatial

rotation, expressed by three time-dependent angles (so-called Euler angles) [1]. Since these angles would change very fast with time and because of the scientific purpose of studying geophysical phenomena, the transformation is favourably specified by a sequence of rotation matrices. The conventional systems used are the International Celestial Reference System (ICRS) and the International Terrestrial Reference System (ITRS) and their corresponding reference frames. These systems are established and maintained by the IERS (International Earth Rotation and Reference Systems Service). The two transformations in use are either based on the ecliptic and the equator, or the new transformation paradigm making use of the so-called NRO (Non-Rotating-Origin) according to the IAU-resolutions 2000 [2]. Before the adoption of the IAU resolutions 2000, polar motion referred to the so-called Celestial Ephemeris Pole (CEP). The CEP was defined such that there are no nearly diurnal motions of this celestial pole with respect to either the space-fixed or the body-fixed system. Along with the new transformation paradigm the CEP was replaced by the Celestial Intermediate Pole (CIP). Its definition is an extension of that of the CEP in the high frequency domain and coincides with that of the CEP in the low frequency domain (for the exact definition we refer to [3]). The concept of the CIP is realized within the IAU 2000A Precession-Nutation Model. The transformation based on ecliptic and equator is shortly described in the following because it is still used in most of the software packages related to the analysis of observation data from space geodetic techniques. In this representation the transformation is performed by the following sequence of rotation matrices [4]:

$$x_i(t) = P(t)N(t)R_3(-\theta(t))R_1(y_p(t))R_2(x_p(t))x_e(t) \quad (1a)$$

$$\text{with } N(t) = R_1(-\varepsilon_A)R_3(\Delta\psi)R_1(\varepsilon_A + \Delta\varepsilon) \quad (1b)$$

$x_i(t)$ and $x_e(t)$ are vectors in the celestial and in the terrestrial reference system, respectively. Both precession matrix $P(t)$ and nutation matrix $N(t)$ describe the change of the direction of the Earth axis in space; the matrix of sidereal time $R_3(-\theta)$ represents the actual rotation angle of the Earth, and the polar motion matrix $W = R_1(y_p(t))R_2(x_p(t))$ indicates the position of the Earth axis with respect to the Earth-fixed reference system, where $x_p(t)$ and $y_p(t)$ are the coordinates of the CIP in the Earth-fixed reference system (ITRS) at time t . The obliquity of the ecliptic is denoted by ε_A , and $\Delta\varepsilon$ and $\Delta\psi$ designate nutation in obliquity and longitude. The actual

rotation of the Earth around the CIP is given via the true sidereal time in Greenwich θ (Greenwich Apparent Sidereal Time: GAST). The true sidereal time is deduced from the mean sidereal time (GMST) considering nutation corrections. UTC is converted to UT1 by applying dUT1, which can be observed by space geodetic techniques. GMST can be derived from UT1 by a definite formula [5]. The five quantities x_p , y_p , $UT1 - UTC = dUT1$, $\Delta\varepsilon$ and $\Delta\psi$ represent the Earth orientation parameters mentioned above. It is necessary to evaluate this transformation between the terrestrial and the celestial reference system in all space-based geodetic analyses, because the observations are made between objects of which the coordinates vary in one system and change slowly, or not at all, in the other system. A stable realisation of the systems along with high-precision observation data from space geodetic techniques gives thus access to high-quality Earth rotation parameters and their variations.

The major effects, detectable in the ERP time series, result from deformations of the solid Earth, mass displacements and fluctuations in oceans and atmosphere and from the interactions between these systems. Mass displacements cause changes of the inertia tensor of the Earth (mass- or pressure-terms), whereas mass motions relative to the reference system alter the relative angular momentum (motion- or wind-terms). The Earth principal moments of inertia are moreover changed periodically due to the reactions of the oceans and the solid Earth to the tidal potential exerted by the Moon and Sun. These variations of the inertia tensor translate into the position of the rotation axis (PM) as well as in the Earth spin rate (LOD) and its total rotational phase angle (UT1).

In the following we describe the derivation of ERP time series from observations of the Global Positioning System (GPS) and of Very Long Baseline Interferometry (VLBI). Subsequently, the variations in the ERP series are examined for periods from a few hours up to 32 days, focusing on signals excited by solid Earth and ocean tides.

2. Determination of Earth rotation parameters

The determination of ERP is typically solved by means of least squares adjustment or Kalman-filtering. The Earth orientation parameters are estimated from the observations of space geodetic techniques, mostly together with numerous other parameters, such as satellite orbits, station coordinates or troposphere parameters.

| Geodetic Parameters | VLBI | GPS, GLONASS | DORIS | SLR | LLR |
|--|------|-----------------|-------|-----|-----------------|
| Position of the Quasars | X | | | | |
| Satellite orbit parameters | | X | X | X | |
| Lunar orbit parameters | | | | | X |
| Nutation | X | X ^{*)} | | | X ^{*)} |
| Polar motion | X | X | X | X | X |
| UT1 | X | | | | X |
| Length of day | X | X | X | X | |
| Station coordinates, Station velocities | X | X | X | X | X |

^{*)} ... only nutation rates can be determined by these techniques

Table 1: Parameters relating to Earth rotation from different space geodetic techniques (taken from [4])

GLONASS – Global'naya Navigatsionnaya Sputnikowaya Sistema

DORIS – Doppler Orbitography Radiopositioning Integrated by Satellite

SLR – Satellite Laser Ranging, LLR – Lunar Laser Ranging

Nutation parameters are thereby, in any case, estimated as corrections to an a priori model. The most current and accurate model is the IAU2000A precession-nutation model. There are essential distinctions between the space geodetic techniques to be considered, w.r.t. the determination of EOP, depending on whether the technique observes satellites or quasars. Because of the necessity to determine orbital elements simultaneously to the EOP, satellite techniques cannot determine dUT1 and nutation offsets directly, but only their temporal changes (rates) [6]. VLBI observations enable to directly estimate dUT1 and nutation offsets, but because of the lack of continuous observations it is more difficult to determine rates. Unfortunately, due to economic and logistic factors, a continuous monitoring of Earth rotation by VLBI is at present not feasible. Polar motion can be determined likewise from both of the mentioned techniques. Table 1 gives an outline of all space geodetic techniques and their ability to determine geodetic parameters related to Earth rotation.

2.1. GPS ERP series

A globally distributed network of stations is a prerequisite to derive ERP from GPS observations. Hence it is indispensable to use automated processing, in order to cope with the huge amount of data. All estimations were therefore performed with the Bernese Processing Engine (BPE) of Bernese GPS Software Version 5.0. The required observation data is kindly provided by the

International GNSS Service (IGS) [7]. Our processing network consists of 113 carefully chosen and fairly stable stations, which belong to the IGS05 reference frame. The network, including the used standard baseline configuration is shown in figure 1. The red lines designate baselines ≤ 2000 km, which are accented here, because the ambiguity resolution is working best for baselines up to this length. By processing data of the year 2005 we derived a year-long ERP series. Since the processing of large GPS networks is very time consuming, and because of limited computing capacities, it was not yet possible to compute longer ERP time series. ERP were set up as continuous piecewise-linear functions at hourly and 6-hours intervals, and were solved for weekly solutions. In the Bernese GPS Software the ERP series are computed by default with respect to a sub-daily ERP model for ocean tide corrections. In our study the Eanes model was used, which is recommended in the IERS Conventions 2003 [8]. The geodetic datum definition uses a minimum constraint solution, imposing a no-net-rotation condition on the station coordinates from IGS05.snz [9]. As orbit information, final orbits of the CODE (Center for Orbit Determination in Europe [10]) were taken and held fixed in the least squares adjustment. We chose to take a priori ERP information from CODE for consistency reasons, since the CODE products were also processed with the Bernese GPS Software. All calculations were performed using absolute antenna phase center corrections. Site displacements due to

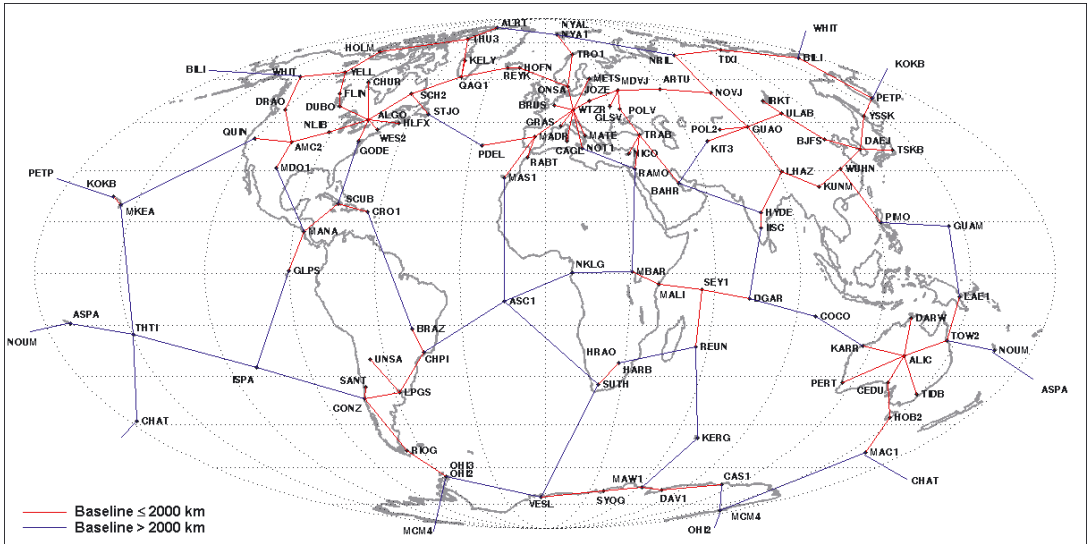


Figure 1: GPS processing network.

ocean loading were taken into account with the FES2004 model. Nutation was modelled using IAU2000A according to the IERS Conventions 2003.

2.2. VLBI ERP series

All estimations of VLBI-based ERP were computed with the VLBI software OCCAM Version 6.1. OCCAM is a research and development package for the analysis of geodetic and geodynamic VLBI experiments. The ERP series generated for this study uses the observation data of all geodetic 24-hour experiments carried out from the beginning of 2000 to the end of 2005 and the so-called Intensive sessions with duration of one hour. Sessions which are not suitable for reliable EOP determination due to their limited extension in one or more components were excluded, as suggested in [11] by the Analysis Coordinator of the IVS (International VLBI Service for Geodesy and Astrometry). The observation data of these measurements is provided by the IVS and available via ftp-download.

The applied reference frame for the VLBI-derived series is the global VLBI solution IGG05R01 [12] of the Institute of Geodesy and Geophysics in Vienna which is a Special Analysis Center of the IVS. Coordinates of stations and sources are fixed to the IGG05R01 frame. Hence the estimates are Earth orientation, troposphere, and clock parameters. Within the processing of the 24-hour experiments nutation offsets, PM and

dUT1 were set up once per session. When processing Intensive sessions, nutation and PM have to be fixed a priori values and solely one dUT1 value is estimated per session. The same a priori nutation model used for the GPS solutions was also applied in VLBI analysis. Site displacements due to ocean loading were modelled based on the ocean tide model GOT00.2. An ERP-series with sub-daily resolution from VLBI observation data is not presented here because this approach demands for another processing strategy, which is still under development.

3. Investigation of Earth rotation variations

The objective of this study was to examine the variations of Earth rotation parameters induced by tidal fluctuations.

3.1. Diurnal and sub-diurnal tidal variations in PM and LOD

The driving forces for the Earth rotation variations of short periods are the changes in ocean heights and currents, which are driven by the tidal acceleration due to the Sun and Moon. Additionally, also atmospheric excitation of PM and dUT1 has to be expected at diurnal and semidiurnal frequencies. Since the excitation of Earth rotation by diurnal and semidiurnal ocean tides is up to two orders of magnitude larger than the corresponding atmospheric influence [13], this aspect will not be treated in the present work. As previously mentioned, sub-daily GPS-derived ERP were estimated w.r.t. a sub-daily model for ocean tide

corrections. Thus the model values were re-applied to the GPS-based ERP series for the analysis. In order to investigate daily and sub-daily variations, the low-frequency variations were removed by subtracting a smooth ERP series, based on the C04 series of the IERS. The Figures 2a-2c show amplitude spectra of the GPS-derived x_p and y_p series and of the GPS-derived LOD series. The spectra for the GPS ERP variations were generated using the CLEAN-algorithm according to [14].

The most distinct peaks in the frequency content of the GPS-based ERP variations are the eight major ocean tidal terms: Q1, O1, P1, and K1 in the diurnal and N2, M2, S2, and K2 in the semidiurnal band. The P1 and K2 peaks have been magnified in the pictures in order to visualise that these terms are separated from K1 and S2, respectively. In a first approach we estimated amplitudes of the eight major ocean tides from the set of GPS-derived ERP. The amplitudes were determined in a least squares adjustment using the following representation for the tidally driven variations:

$$\Delta X(t) = \sum_{j=1}^n [sx_j \sin \varphi_j(t) + cx_j \cos \varphi_j(t)] \quad (2a)$$

$$\Delta Y(t) = \sum_{j=1}^n [sy_j \sin \varphi_j(t) + cy_j \cos \varphi_j(t)]$$

$$\Delta LOD(t) = \sum_{j=1}^n [sl_j \sin \varphi_j(t) + cl_j \cos \varphi_j(t)]$$

$$\varphi_j(t) = \sum_{i=1}^6 N_{ij} F_i(t) \quad (2b)$$

$\Delta X(t)$, $\Delta Y(t)$ and $\Delta LOD(t)$ denote the observed tidal variations in the corresponding quantities; the sx_j , cx_j , sy_j , cy_j , sl_j and cl_j are the corresponding sine and cosine amplitudes, while n specifies the number of tides considered. The angle argument $\varphi_j(t)$ is built as a linear combination of the five fundamental arguments and GMST + π ; as the sixth argument (see [8]). Each tide j is thereby characterized by a special sequence of integer multipliers N_{ij} .

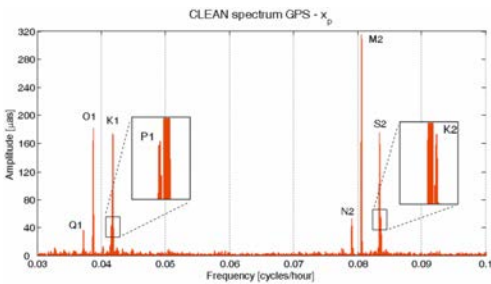


Figure 2a: CLEAN spectrum of the diurnal and sub-diurnal tidal frequency bands from GPS-derived x_p time series.

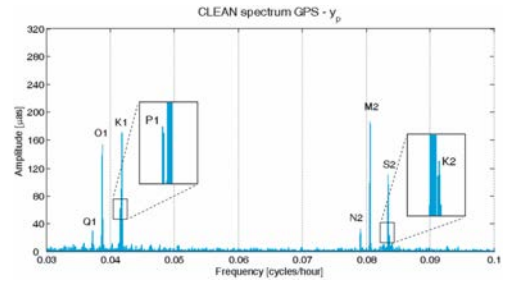


Figure 2b: CLEAN spectrum of the diurnal and sub-diurnal tidal frequency bands from GPS-derived y_p time series.

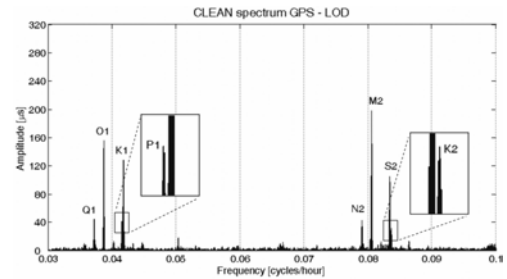


Figure 2c: CLEAN spectrum of the diurnal and sub-diurnal tidal frequency bands from GPS-derived LOD time series.

In the tables 2a–c the sine and cosine amplitudes of the tidal variations from our estimate are compared to the sum of the corresponding IERS amplitudes and the amplitudes of those neighbouring periods, which differ by one cycle only after a full revolution of the lunar node. The current IERS model for ERP variations caused by ocean tides is an extension of the model calculated by Ray [15] from Satellite Altimetry data. The modulus of the amplitudes estimated in the least squares adjustment agrees to the magnitude of the constituents found by the CLEAN-algorithm within three times the formal error of the adjustment. When we compare the estimated signal magnitudes to the values of the IERS model the overall agreement is about 50% (the last row of each table gives the difference of the absolute values of the observed amplitudes minus the combined model amplitudes). With three times the formal error as a criterion the least accordance between observations and model is found in the y_p variations, where accordance is given only for the Q1, N2 and M2 terms. For the x_p variations the values agree for the Q1, N2, M2 and K2 tides. The closest agreement arises for the LOD variations, where all terms except the O1 term meet the criterion. The most peculiar

| Period [hours] | Tide | ΔX (observed) Amplitude of | | ΔX (IERS) Comb. amplitude of | | Diff. Amp obs-IERS [μas] |
|----------------|------|------------------------------------|------------------------|--------------------------------------|------------------------|---|
| | | sin [μas] | cos [μas] | sin [μas] | cos [μas] | |
| 26.87 | Q1 | 8.1 \pm 2.4 | 36.1 \pm 2.4 | 7.4 | 31.3 | 4.9 |
| 25.82 | O1 | 53.8 \pm 2.4 | 173.9 \pm 2.4 | 58.0 | 158.0 | 13.7 |
| 24.07 | P1 | 26.8 \pm 2.4 | 38.8 \pm 2.4 | 25.8 | 50.6 | -10.2 |
| 23.93 | K1 | -97.9 \pm 2.4 | -152.8 \pm 2.4 | -86.5 | -169.3 | -8.6 |
| 12.66 | N2 | -54.6 \pm 2.4 | -3.8 \pm 2.4 | -54.8 | -12.4 | -1.4 |
| 12.42 | M2 | -322.1 \pm 2.4 | -21.7 \pm 2.4 | -317.9 | -26.0 | 3.9 |
| 12.00 | S2 | -155.8 \pm 2.3 | 79.7 \pm 2.4 | -144.1 | 63.6 | 17.5 |
| 11.97 | K2 | -60.7 \pm 2.4 | 4.5 \pm 2.4 | -49.9 | 24.9 | 5.1 |

Table 2a: Major ocean tidal terms for ΔX (observed) vs. major ocean tidal terms + sideband terms for ΔX according to IERS.

| Period [hours] | Tide | ΔY (observed) Amplitude of | | ΔY (IERS) Comb. amplitude of | | Diff. Amp obs-IERS [μas] |
|----------------|------|------------------------------------|------------------------|--------------------------------------|------------------------|---|
| | | sin [μas] | cos [μas] | sin [μas] | cos [μas] | |
| 26.87 | Q1 | -29.7 \pm 2.5 | 4.8 \pm 2.5 | -31.3 | 7.4 | -2.1 |
| 25.82 | O1 | -148.1 \pm 2.5 | 42.5 \pm 2.5 | -158.0 | 58.0 | -14.3 |
| 24.07 | P1 | -60.7 \pm 2.5 | 23.5 \pm 2.5 | -50.6 | 25.8 | 8.3 |
| 23.93 | K1 | 153.2 \pm 2.4 | -97.3 \pm 2.5 | 169.3 | -86.5 | -8.6 |
| 12.66 | N2 | 10.8 \pm 2.5 | 32.0 \pm 2.5 | 10.7 | 30.8 | 1.2 |
| 12.42 | M2 | 50.8 \pm 2.5 | 183.5 \pm 2.5 | 36.2 | 188.6 | -1.7 |
| 12.00 | S2 | 68.1 \pm 2.4 | 90.8 \pm 2.5 | 59.2 | 86.6 | 8.6 |
| 11.97 | K2 | 8.4 \pm 2.5 | 22.8 \pm 2.5 | 23.0 | 30.0 | -13.5 |

Table 2b: Major ocean tidal terms for ΔY (observed) vs. major ocean tidal terms + sideband terms for ΔY according to IERS.

| Period [hours] | Tide | ΔLOD (observed) Amplitude of | | ΔLOD (IERS) Comb. amplitude of | | Diff. Amp obs-IERS [μas] |
|----------------|------|--------------------------------------|------------------------|--|------------------------|---|
| | | sin [μas] | cos [μas] | sin [μas] | cos [μas] | |
| 26.87 | Q1 | -13.5 \pm 3.6 | -42.9 \pm 3.6 | -16.7 | -34.1 | 7.0 |
| 25.82 | O1 | -86.8 \pm 3.6 | 129.9 \pm 3.6 | -83.8 | -111.3 | 17.0 |
| 24.07 | P1 | -22.3 \pm 3.6 | -36.4 \pm 3.6 | -19.2 | -34.2 | 3.5 |
| 23.93 | K1 | 63.2 \pm 3.6 | 116.6 \pm 3.6 | 60.1 | 123.9 | -5.1 |
| 12.66 | N2 | -18.2 \pm 3.6 | 40.6 \pm 3.6 | -17.9 | 43.5 | -2.5 |
| 12.42 | M2 | -90.6 \pm 3.6 | 179.8 \pm 3.6 | -83.6 | 189.2 | -5.6 |
| 12.00 | S2 | 3.0 \pm 3.6 | 105.6 \pm 3.6 | -2.0 | 94.8 | 10.8 |
| 11.97 | K2 | -5.5 \pm 3.6 | 32.0 \pm 3.7 | 0.7 | 34.4 | -2.0 |

Table 2c: Major ocean tidal terms for ΔLOD (observed) vs. major ocean tidal terms + sideband terms for ΔLOD according to IERS.

difference results in the variations of all three parameters for the O1 term, which is with the exception of x_p , larger than for the other terms. It is not probable that these differences are technique specific artefacts since the regarded tide is not close to any resonance frequency of the satellite revolution period. To what extent the observed differences are deficiencies in the IERS model has to be investigated on the basis of a longer time series and compared to results of a second time series, gained from another technique, such as VLBI. For the future, it is intended to scrutinize the ERP variations (derived from both techniques) for non-tidal signals as well, and to solve for an extended set of ocean tide amplitudes, including the sidebands. Therefore it will be necessary to constrain the ratio of the sideband amplitude and the amplitude of the major tide (see [16] for further information).

3.2. Long-period tidal variations in dUT1/LOD

The second point of interest of our work is the impact of zonal Earth tides on the rotation of the Earth. The deformations of the Earth, caused by the zonal part of the tidal potential, periodically change the principal moments of inertia. This leads in accordance to the conservation of angular momentum to periodic changes in the rotation speed and thus in dUT1 and LOD. The variations show periods from ~5 days to 18.6 years. For the investigation of these effects we used a continuous one-year GPS LOD series with a 6-hour resolution and a six year VLBI dUT1 series, given in daily intervals, except for time periods where no measurements were available. We estimated the amplitudes of 10 terms from the LOD series and of 12 terms from the dUT1 series at fixed periods. Periods are given in units of days: 6.86, 7.10, 9.13, 9.56, 12.81, 13.66, (13.78), 14.77, 23.94, (27.09), 27.56, 31.81. The amplitudes for the periods in braces were estimated from the dUT1 series only, because these terms would not be separable from the one-year LOD time series. One term (at 12.81 days) was added with the amplitude expected to be around zero, for testing the correctness of the approach. The observation equations were set up quite similar as for the estimation of the ocean tide amplitudes, with the exception that only the five fundamental arguments are used in this approach. The representation reads as follows:

$$\delta UT1(t) = \sum_{j=1}^n [B_j \sin \varphi_j(t) + C_j \cos \varphi_j(t)] \quad (3a)$$

$$\delta LOD(t) = \sum_{j=1}^n [B'_j \cos \varphi_j(t) + C'_j \sin \varphi_j(t)]$$

$$\varphi_j(t) = \sum_{i=1}^5 N_{ij} F_i(t) \quad (3b)$$

Actually we solved only for the B amplitudes and neglected the so-called out-of-phase terms, which are denoted as C amplitudes here, because their magnitude is close to zero, according to the model currently recommended by the IERS [17].

For the derivation of the amplitudes corresponding to periods <32 days it was necessary to filter tidal signals of longer periods and strong atmospheric signals from the original data. The influence of the atmosphere was reduced using atmospheric angular momentum data of the NCEP (U.S. National Centers for Environmental Prediction) [18]. Additionally we subtracted the term at 13.63 days, since it is of reasonable size and strongly correlates to the term at 13.66 days. At least 18.6 years of data would be required to separate these two periods. The remaining low-frequency signal was removed by applying a highpass filter. Figures 3a and 3b display the frequency content of the LOD and dUT1 signals after the filtering process.

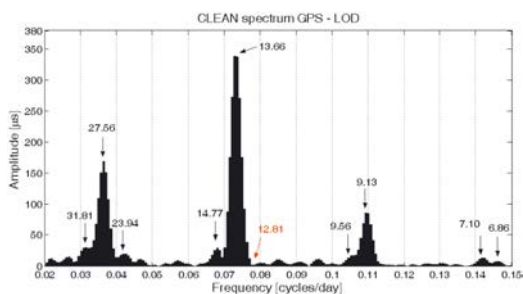


Figure 3a: CLEAN spectrum of filtered GPS-derived LOD time series with periods given in days.

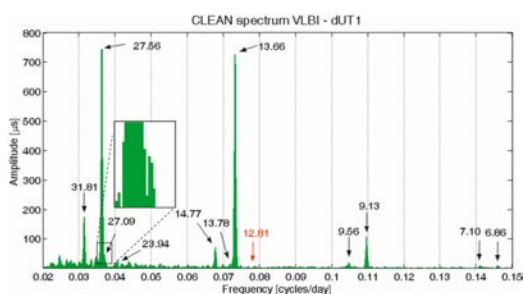


Figure 3b: CLEAN spectrum of filtered VLBI-derived dUT1 time series with periods given in days.

It can be seen that the 9 resp. 11 terms sought for are existent in the spectra and that there is almost no signal at the period 12.81 days with the expected zero amplitude. There is small signal content remaining also at non-tidal periods, such as between 10–12 days, 15–22 days and over 32 days. These peaks are most probably the results of insufficient modelling of the atmospheric influence.

Both, the GPS-derived LOD variations and the VLBI-derived dUT1 variations were additionally subjected to a second spectral analysis based on a heuristic method [19]. The purpose of the heuristic analysis is not to estimate the amplitudes at predefined periods but to determine the periods with the largest amplitudes. Calibrated for the search of 9 periods (in the range of 5 to 32 days), the algorithm found amplitude maxima in the LOD variations at the following periods: 31.81, 31.63, 27.37, 23.66, 14.74, 14.17, 13.65, 9.47 and 9.12 days. When restricting the search range to below 8 days also peaks at the periods 7.06 and 6.44 days can be found. But they are obviously of less energy than the unexpected peaks at 23.66 and 14.17 days. A small tidal constituent would be expected at 23.94 days, but it is already visible in the amplitude spectrum (Figure 3a) that there is significantly more signal around this period than predicted from the IERS model. The origin of this oversized peak is not quite clear, but we assume that it is also due to insufficient modelling of atmospheric influence. The detected peak at 14.17 days is possibly the result of an aliasing of the residual diurnal tidal signature of the O1 tide to this period. This effect has been observed in GPS height time series so far [20] and has to be investigated for LOD series in further studies.

With the constraint to search for 11 peaks (between 5 and 32 days), the following periods resulted from the heuristic analysis of the dUT1 variations: 31.79, 29.89, 28.84, 27.91, 27.54, 26.93, 24.56, 14.76, 13.78, 13.66 and 9.13 days. Again, when we limit the search range to below 10 days also peaks at 9.54, 7.09 and 6.86 days are found. As the algorithm detects periods corresponding to amplitude maxima we have to state that these results are congruent to the CLEAN spectral analysis (Figure 3b), where we clearly see the signal content between 30 and 27.6 days. The occurrence of these peaks and also of the peak at 24.56 days is also supposed to be the consequence of the subtraction of mismodeled atmospheric excitation.

Table 3 shows our results of the least squares estimation on the left hand side. On the right side the zonal tidal terms for the estimated periods plus neighbouring periods are given according to the IERS Conventions 2003 [8]. The estimated terms result as a combined amplitude of the principal and the sideband terms. With three times the estimation error as a criterion and taking into account also the contribution of the sideband amplitudes the majority of the estimated terms agrees with the values of the IERS model. In both cases this does not hold for the terms 9.13 and 13.66 days, where the estimated amplitudes are smaller than the combined amplitudes predicted from the model. For the dUT1 variations also the estimated terms at 27.09, 27.56 and 31.81 do not match the combined terms of the IERS model. This mismatch, especially in the case of the dUT1 variations where we investigated a time series of six years, gives rise to the question if it is adequate to compare the estimates simply with the sum of the amplitudes of the considered periods and their sidebands. It might be more appropriate for the analysis of a time series of this length to constrain the sideband amplitudes and estimate them as well. The smaller size of the fortnightly terms could be a consequence of not reducing the long-period ocean tide (treated for example in [21]), which is existent at the same period but with a different phase.

| VLBI δUT1 | | | IERS δUT1 | | GPS δLOD | | | IERS δLOD | |
|------------|----------|----------|------------|----------|------------|----------|----------|------------|----------|
| Period [d] | Sin [μs] | RMS [μs] | Period [d] | Sin [μs] | Period [d] | Cos [μs] | RMS [μs] | Period [d] | Cos [μs] |
| | | | 6.85 | -4.0 | | | | 6.85 | 3.8 |
| 6.86 | -13.9 | 3.9 | 6.86 | -10.0 | 6.86 | 9.5 | 2.5 | 6.86 | 9.1 |
| | | | 7.09 | -5.0 | | | | 7.09 | 4.5 |
| 7.10 | -10.3 | 3.9 | 7.10 | -12.0 | 7.10 | 11.9 | 2.5 | 7.10 | 10.9 |
| | | | 9.12 | -41.0 | | | | 9.12 | 28.4 |
| 9.13 | -102.9 | 3.9 | 9.13 | -100.0 | 9.13 | 87.4 | 2.5 | 9.13 | 68.5 |
| | | | 9.54 | -8.0 | | | | 9.54 | 5.4 |
| 9.56 | -19.3 | 3.9 | 9.56 | -20.0 | 9.56 | 15.8 | 2.5 | 9.56 | 13.0 |
| 12.81 | 8.5 | 3.9 | 12.81 | 2.0 | 12.81 | -2.7 | 2.5 | 12.81 | -1.1 |
| 13.66 | -740.3 | 3.9 | 13.66 | -779.0 | 13.66 | 349.1 | 2.5 | 13.66 | 358.4 |
| 13.78 | -26.5 | 3.9 | 13.78 | -34.0 | | | | | |
| | | | 14.73 | 5.0 | | | | 14.73 | -2.0 |
| 14.77 | -75.1 | 3.9 | 14.77 | -74.0 | 14.77 | 28.9 | 2.5 | 14.77 | 31.4 |
| | | | 14.80 | -5.0 | | | | 14.80 | 2.2 |
| | | | 23.86 | 5.0 | | | | 23.86 | -1.3 |
| 23.94 | 6.0 | 3.9 | 23.94 | 10.0 | 23.94 | -3.8 | 2.5 | 23.94 | -2.6 |
| | | | 26.98 | 18.0 | | | | | |
| 27.09 | 37.5 | 3.9 | 27.09 | 44.0 | | | | | |
| | | | 27.44 | 54.0 | | | | 27.44 | -12.3 |
| 27.56 | -774.7 | 3.9 | 27.56 | -833.0 | 27.56 | 168.6 | 2.5 | 27.56 | 189.9 |
| | | | 27.67 | 55.0 | | | | 27.67 | -12.5 |
| | | | 31.66 | 12.0 | | | | 31.66 | -2.4 |
| 31.81 | -171.6 | 3.9 | 31.81 | -184.0 | 31.81 | 31.3 | 2.5 | 31.81 | 36.3 |
| | | | 31.96 | 13.0 | | | | 31.96 | -2.6 |

Table 3: Zonal tidal terms.

4. Conclusions and Outlook

We investigated Earth rotation variations at tidal frequencies on the basis of GPS- and VLBI-derived Earth rotation parameters. The estimated ocean tide amplitudes are regarded as preliminary results, since fairly longer time series would be necessary to provide robust and reliable solutions. A comparable parallel computation of the ocean tidal terms from VLBI-derived ERP would essentially improve the reliability. Before this intention can be put into practice though, we will still have to focus on the derivation of high-quality sub-daily ERP from VLBI observations. Concerning the obtained zonal tidal terms for LOD and dUT1 we conclude that the magnitudes agree quite well with the values predicted by the IERS model. But as mentioned above, the way of comparison has to be reconsidered and the adjustment model needs to be modified accordingly. Additionally, it is intended to investigate the effect of the long-period ocean tides. In general it is definitely desirable to refine the method of removing non-tidal signals, such as the atmospheric influence and to generate ERP time series which allow for the separation of all adjacent periods and the estimation of periods >32 days. Thus, it would be possible to avoid affecting the observed signal by a priori model information and thereby to resolve the source of the hitherto inscrutable peaks at periods of around 30 and 28 days in the dUT1 variations from VLBI and around 24 days in the LOD variations from GPS. Interesting conclusions will be feasible also from the analysis of combined GPS-VLBI ERP series, an important objective of our future work.

Acknowledgements

The main author is grateful holder of a DOC-FFORTE dissertation grant of the Austrian Academy of Sciences. We appreciate the valuable comments of the reviewers, which contributed to the improvement of this article.

References

- [1] *Moritz H. and Mueller I.I. (1987):* Earth Rotation, Theory and Observation. The Ungar Publishing Company, New York.
- [2] IAU-Resolutions 2000, http://syrite.obspm.fr/IAU_resolutions/Resol-UA1.htm
- [3] *Capitaine N. (2000):* Definition of the Celestial Ephemeris Pole and the Celestial Ephemeris Origin. Towards models and constants for sub-microarcsecond astrometry, Proceedings of IAU Colloquium 180 held at the U.S. Naval Observatory, Washington, DC, USA, 27-30 March 2000, Washington, DC: U.S. Naval Observatory, 2000 xix, 427 p. Edited by Kenneth J. Johnston, Dennis D. McCarthy, Brian J. Luzum, and George H. Kaplan., p. 153
- [4] *Schuh H., Dill R., Greiner-Mai H., Kutterer H., Müller J., Nothnagel A., Richter B., Rothacher M., Schreiber U. and Soffel M. (2003):* Erdrotation und globale dynamische Prozesse. Mitteilungen des Bundesamtes für Kartographie und Geodäsie, Band 32. Verlag des Bundesamtes für Kartographie und Geodäsie, Frankfurt am Main.

- [5] *Schödlbauer A. (2000):* Geodätische Astronomie. Walter de Gruyter, Berlin.
- [6] *Rothacher M., Beutler G., Herring T.A. and Weber R. (1999):* Estimation of Nutation using the Global Positioning System. Journal of Geophysical Research, Vol. 104, NO. B3, p. 4835–4859.
- [7] IGS: <http://igs.cb.jpl.nasa.gov/>
- [8] IERS Conventions (2003). Dennis D. McCarthy and Gérard Petit. (IERS Technical Note; 32). Verlag des Bundesamtes für Kartographie und Geodäsie, Frankfurt am Main.
- [9] ftp://igs.cb.jpl.nasa.gov/igs_cb/station/coord/IGS05.snx
- [10] <ftp://ftp.unibe.ch/aiub/CODE/>
- [11] <http://vlbi.geod.uni-bonn.de/IVS-AC/data/exclude.txt>
- [12] *Heinkelmann R., Boehm J., Schuh H. and Tesmer V. (2006):* Global VLBI solution IGG05R01, in IVS 2006 General Meeting Proceedings, edited by D. Behrend and K.D. Baver, NASA/CP-2006-214140, 2006.
- [13] *Brzezinski A., Bizouard Ch. and Petrov S.D. (2002):* Influence of the Atmosphere on Earth Rotation: what new can be learned from recent atmospheric angular momentum estimates? Surveys in Geophysics, 23, p. 33–69.
- [14] *Baisch S. and Bokelmann G.H.R. (1999):* Spectral analysis with incomplete time series: an example from seismology. Computers & Geosciences, 25, p. 739–750.
- [15] *Ray R.D., Steinberg D.J., Chao B.F., Carthwright D.E. (1994):* Diurnal and Semicircular Variations in the Earth's Rotation Rate Induced by Oceanic Tides. Science, 264, p. 830–832.
- [16] *Gipson J.M. (1996):* Very long baseline interferometry determination of neglected tidal terms in high-frequency Earth rotation variation. Journal of Geophysical Research, Vol. 101, NO. B12, p. 28,051–28,064.
- [17] *Defraigne P. and Smits I. (1999):* Length of day variations due to zonal tides for an inelastic earth in non-hydrostatic equilibrium. Geophysical Journal International, 139, p. 563–572.
- [18] *Salstein D.A. and Rosen R.D. (1997):* Global momentum and energy signals from reanalysis systems. 7th Conf. on Climate Variations, American Meteorological Society, Boston, MA, p. 344–348.
- [19] *Mautz R. (2001):* Zur Lösung nichtlinearer Ausgleichungsprobleme bei der Bestimmung von Frequenzen in Zeitreihen. Dissertation, Fachbereich 9 – Bauingenieurwesen und Angewandte Geowissenschaften der Technischen Universität Berlin.
- [20] *Penna N.T. and Stewart M.P. (2003):* Aliased tidal signatures in continuous GPS height time series. Geophysical Research Letters, Vol. 30, NO. 23, 2184, doi:10.1029/2003GL018828.
- [21] *Kantha L.H. and Stewart J.S. (1998):* Long-period lunar fortnightly and monthly ocean tides. Journal of Geophysical Research, Vol. 103, NO. C6, p. 12639–12647.

Contact

Dipl.-Ing. Sigrid English, Institute of Geodesy and Geophysics, Vienna University of Technology, Gusshausstr. 27-29, 1040 Vienna, Austria. E-mail: senglish@mars.hg.tuwien.ac.at

Dr. Paulo Jorge Mendes Cerveira, Institute of Geodesy and Geophysics, Vienna University of Technology, Gusshausstr. 27-29, 1040 Vienna, Austria. E-mail: mendes@mars.hg.tuwien.ac.at

Dr. Robert Weber, Institute of Geodesy and Geophysics, Vienna University of Technology, Gusshausstr. 27-29, 1040 Vienna, Austria. E-mail: rweber@mars.hg.tuwien.ac.at

Prof. Harald Schuh, Institute of Geodesy and Geophysics, Vienna University of Technology, Gusshausstr. 27-29, 1040 Vienna, Austria. E-mail: hschuh@mars.hg.tuwien.ac.at